The modelling of the generation of volatiles, H_2 and CO, and their simultaneous diffusion controlled oxidation, in pulverized coal furnaces

A. BERMÚDEZ†, J. L. FERRÍN† and A. LIÑÁN§*

The purpose of this paper is to contribute to the mathematical modelling of the combustion of coal particles in pulverized coal furnaces. The model deals with the gas and solid phases of the flow. For the coal particles a Lagrangian description is used, taking into account the simultaneous processes of moisture evaporation and devolatilization together with the heterogeneous gasification reactions of the char.

An Eulerian description will be used for the distributions of temperature and concentrations in the gas phase, with the effect of the particles represented by volumetric sources of heat, mass and momentum. The gas phase oxidation reactions of the volatiles, H_2 and CO will be modelled using the assumption of infinitely fast rates; the Burke–Schumann analysis will be generalized to account for the competition for oxygen of CO, H_2 and the volatiles. These reactions may occur, in the form of group combustion, in a gaseous thin diffusion flame separating a region without oxygen, where the coal particles generate volatiles, H_2 and CO, from a region with oxygen, where the reactions may occur inside the particles or, outside, in diffusion flames surrounding the individual particles, even though for small particle sizes the gas phase reactions can be considered as frozen near the particles.

The analysis will provide relations for the volumetric sources appearing in the gas phase description, and for the rates that determine the evolution of the temperature and mass content of moisture, volatiles and char in the particles.

Keywords: Char gasification; CO combustion; Group combustion; Pulverized coal; Pulverized flames

1. Introduction

The combustion of coal particles has been extensively treated in the literature due to its role in fluidized bed and pulverized coal furnaces; see for example Saxena [1] and references therein. Our aim is to contribute to the modelling of the combustion of individual porous coal particles in their local gas environment, which results from the collective effects of the particles in pulverized coal furnaces.

Coal particles enter the furnace transported by primary air through injectors, with an additional co-flow of air (see figure 1). In a first stage the particles, after being heated mainly

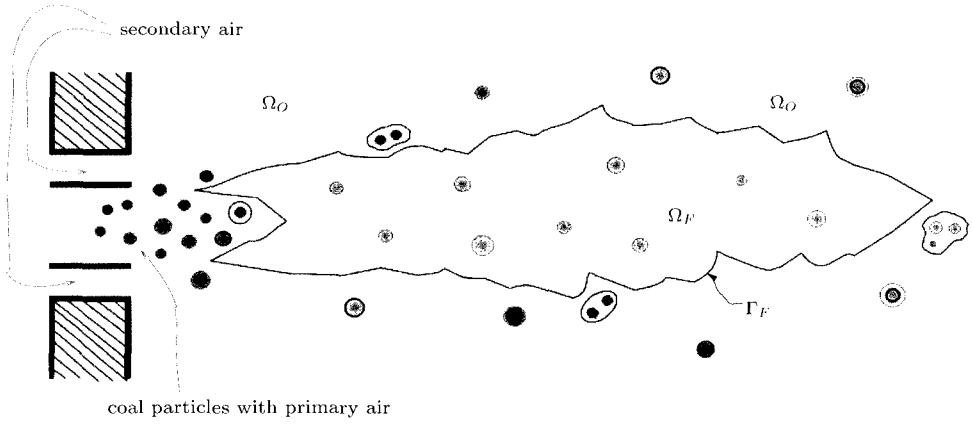

Figure 1. Diffusion flame. Boldface circumferences and lines represent the flame sheets.

by radiation, undergo moisture evaporation and devolatilization of species, which will later react with oxygen. The remaining carbon, or char, is gasified by heterogeneous reactions with either CO_2, O_2 or H_2O to generate CO and H_2 that will burn in the gas phase.

The classical papers by Nusselt [2] and Burke and Schumann [3] can be considered as the first important contributions to the field from a theoretical point of view. In the former, Nusselt assumes that direct oxidation of carbon by oxygen occurs only at the surface of the particle. In the latter, Burke and Schumann assume that carbon is consumed by CO_2 at the surface, while the CO thus formed reacts with O_2 at a flame sheet to form CO_2.

A comprehensive theoretical description of the combustion of a single coal particle in an oxidizing ambient was given by Libby and Blake [4] and Libby [5]. With the aim of calculating the combustion rate they account in the conservation laws and boundary conditions for the effect of three chemical reactions, two heterogeneous at the surface of the particle and one homogeneous in the gas neighbourhood of the particle.

When analysing the gasification and combustion of coal particles in pulverized coal combustion chambers the gasification process is often modelled as pyrolysis reactions that generate water vapour and other volatile fuels containing mainly C, H and S. The carbon contained in the remaining char is gasified, mainly after devolatilization, by a surface reaction with oxygen, to generate CO, or with CO_2 or H_2O, also to generate CO and H_2. In non-porous particles these heterogeneous reactions could take place only on the external surface of the particle. However, in coal particles with significant initial mass fractions of humidity and volatiles the reactions would take place inside the particle at the internal surface of the pores. We shall be mainly concerned with the combustion of particles with a significant content of ashes, so that a non-burning fraction of the original coal particle is left in the form of a porous solid residue.

In the gas phase, the volatiles, H_2 and CO compete for the O_2 they need for their oxidation to CO_2, H_2O and SO_2. In the analysis that follows we shall account for finite rate effects when describing the kinetically controlled heterogeneous gasification reactions, which become diffusion controlled for high particle temperatures. However we shall consider the gas phase reactions to be very fast, following the procedure introduced by Burke and Schumann [3], and thus occurring in a diffusion controlled way inside the particles or in flame sheets outside. When the size of the particle is small, the gas phase reactions, which can be considered to be frozen inside or in the vicinity of the particles, will take place in more extended regions in the near wake of the particle, with small values of the mass fractions of the volatiles, CO and H_2 and without preventing the oxygen to reach the particle and participate in the char oxidation.

Finite rate effects determine the conditions allowing for the gas phase reactions to be considered as frozen or infinitely fast. The description of the conditions for the transition between the frozen and equilibrium modes of combustion of a single particle in a oxidizing gas environment was given by Matalon [6–8], in terms of particle size based Damköhler numbers, following the method of large activation energies used by Liñán [9] in his analysis of the ignition and extinction of diffusion flames. In Makino and Law [10] an ignition criterion for the CO flame is obtained. Finally, approximate explicit expressions for the combustion rate are obtained by Makino [11]. We shall give below and in Section 3 additional considerations concerning the conditions for diffusion controlled combustion in flame sheets.

The fact that we consider three reactants – the volatiles, H_2 and CO – competing for the oxygen, forces us to generalize the Burke–Schumann procedure, using Schvab–Zeldovich variables, to account for this competition. This has to be done (see Section 5) in a way that will enable us to calculate explicitly the temperature and the concentration of all of the reactants and products.

The small values of the coal particle volumetric fraction allow us to carry out a homogenized analysis of the combustion process of the gas particle mixture. We shall use a Lagrangian description for the evolution of the coal particles in a gaseous environment of varying temperature and composition. This corresponds to the particle source in cell (PSI-Cell) model of typical turbulent combustion codes, used for example by Smith *et al.* [12]. When describing the gas phase distributions of the mean field concentrations and temperature, we shall use an Eulerian description, accounting in the conservation equations for the effects of the gas phase oxidation of CO, H_2 and of the volatiles, and also for the sources of mass and energy due to the gasification and combustion of the particles at each computing cell used in the Eulerian gas phase description. These sources of energy and mass are provided by the Lagrangian analysis of the response of the particles passing through the cell. Their motion as well as their combustion rate at each instant will be determined by the temperature and composition of the ambient gas around them. Hence there exists a bi-directional coupling between the two models for the gas and solid phases.

The validity of the model is dependent on the inequalities $L \gg l_c \gg l_p \gg a$, between the length scales, L of the burner, l_c of the computational cell, l_p of the interparticle distance and a the radius of the coal particle (see the review by Annamalai and Ryan [13]).

When describing the particle response we shall account for the combined effects of the devolatilization reactions producing water vapour and reacting volatiles, and the char oxidation reactions, allowing for, as in Gurgel Veras *et al.* [14], the overlapping of the reactions. As we shall see below, the particle response depends on whether or not the oxygen in the cell has been depleted by the gas phase oxidation reactions.

For the description of the gas phase reactions we shall use the Burke–Schumann assumption of infinitely fast reactions, that prevents the coexistence of oxygen with the reactants (volatiles, CO and H_2). Then we find two regions, Ω_O and Ω_F, in the homogenized gas (see figure 1). In Ω_F there is no oxygen, and in Ω_O there are no reactants in the homogenized gas phase. The gas phase reactions occur in the form of diffusion controlled group combustion in a flame sheet Γ_F that separates Ω_F from Ω_O; this gaseous diffusion flame is distorted by the turbulent flow.

When observing the diffusion flame, before homogenization, we will see a wrinkling of the flame associated to the fine graining due to the individual particles and, also, combustion in clusters of two or several particles, close to the main continuous diffusion flame where the oxygen concentration is low. However, the homogenization process eliminates these fine graining effects, which on the other hand are not very important.

The validity of the Burke–Schumann assumption when describing the homogenized gas phase is based on the criterium that the Damköhler number, or ratio of the gas turbulent mixing time and the chemical time is large compared to unity; a requirement easier to satisfy

than the requirement that the particle based Damköhler number is large. In this last case, to be consistent with the assumption of infinitely fast reactions, we must also take into account that the gas phase reactions may also occur in the region Ω_O in the form of flame sheets inside the porous particle or outside, surrounding the individual particles. The effects of these reactions must be included in the Lagrangian analysis of the particle response, because they contribute to the O_2 sink and CO_2, H_2O and thermal energy sources entering the Eulerian description of the mean gas variables.

By using generalized Schvab–Zeldovich variables, with the gas phase reactions eliminated, it is possible to decide automatically when we may encounter individual diffusion flames around the particles or when there is diffusion controlled group combustion, even in the cases considered here when there are several species competing for the oxygen in the gas phase.

Our aim in this paper is to generate the form of the conservation laws appropriate for diffusion controlled combustion in the gas phase accounting for the sources provided by the particles lying in the computational cell. We do not address here the modelling problem of generating the equations for the averaged variables of the turbulent flow from the detailed conservation equations, given in this paper, governing the fluctuating variables in the flow. In particular, the modelling of the gas phase source terms due to the reactions when they are diffusion controlled is facilitated by the introduction of presumed forms of the probability density distributions of the coupling functions.

Our goal in this paper is to contribute to the methodology of analysis of the group combustion of coal particles in pulverized coal furnaces when the gas phase reactions times are compared with the diffusion time in the homogenized gas phase.

The transition from frozen flow to diffusion controlled flow can be determined for the Arrhenius kinetics that we use in the formulation. However, for the results to be relevant a more detailed and realistic kinetic description should be used.

Numerical results based in this methodology will be given in future publications.

This paper is organized as follows. The physico-chemical model describing the combustion of a coal particle is presented in Section 2. In Section 3 we proceed with the modelling of the gas phase. The reaction processes taking place within the particles are described in Section 4, while those taking place outside in the neighbourhood of the particles are described in Section 5. Finally Section 6 shows the expressions of the sources to the gas phase resulting from the contribution of the single particles. We conclude with a summary of the model developed in previous sections and with some conclusions.

2. The combustion model

There is a large variety of models for the description of the generation of volatiles and char oxidation, which are a consequence of the complexity of the physical and chemical processes that occur, and also of the large variety of coal types. We shall not attempt either to review these processes (see for example the review by Annamalai and Ryan [15]) or to propose a general mathematical model for the particle evolution. Our goal is to illustrate, using a simple model of volatiles generation and char oxidation, how the Lagrangian evolution of a particle, in the variable temperature and concentration environment that it encounters, provides us with the sources that appear in the conservation equations for the homogenized gas phase.

For simplicity in the presentation, all the volatiles are represented by a single molecule $V_{(g)} = C_{\kappa_1} H_{\kappa_2} O_{\kappa_3} S_{\kappa_4}$ of molecular mass M_{vol}, where the coefficients κ_1, κ_2, κ_3 and κ_4 are deduced from the ultimate analysis of the coal.

We consider a simplified kinetic model consisting of the following physico-chemical processes within the porous particles:

- devolatilization:

$$\underline{4} \qquad V_{(s)} \rightarrow V_{(g)} + (q_4);$$

- evaporation of the absorbed moisture:

$$\underline{5} \qquad H_2O_{(s)} \rightarrow H_2O_{(g)} + (q_5);$$

In addition we have to account for the char oxidation by heterogeneous reactions taking place at the internal surface of the porous particle:

- carbon oxidation by carbon dioxide:

$$\underline{1} \qquad CO_2 + C_{(s)} \rightarrow 2\,CO + (q_1);$$

- carbon oxidation by oxygen:

$$\underline{2} \qquad \frac{1}{2}O_2 + C_{(s)} \rightarrow CO + (q_2);$$

- carbon oxidation by water vapour:

$$\underline{3} \qquad H_2O + C_{(s)} \rightarrow CO + H_2 + (q_3);$$

where the index s refers to the solid phase and g to the gas phase. The q_i denotes the heat released in the i-th reaction per unit mass gasified. The char gasification reaction 3 plays an important role in coal combustion chambers because water vapour is generated with moisture evaporation and in the combustion of the volatiles.

For the generation of volatiles and moisture evaporation we shall use the simple laws

$$w_4 = B_4 e^{-E_4/\mathcal{R}T} \rho_V, \tag{1}$$

$$w_5 = B_5 e^{-E_5/\mathcal{R}T} \rho_{H_2O}, \tag{2}$$

where ρ_V and ρ_{H_2O} are the local values within the coal particle of the density of volatiles and H_2O remaining in condensed form. The moisture generation is for simplicity here described with a kinetic model similar to the pyrolysis model of volatiles generation. We have chosen the rates of water vapour and volatiles generation to be of first order with respect to ρ_{H_2O} and ρ_V.

The rates of the heterogeneous reactions (1, 2 and 3) are modelled in terms of overall intrinsic combustion or gasification rates, per unit internal surface area, that depend on the local temperature and partial pressures of the gas reactants involved in the reaction (see for example the review by Annamalai and Ryan [15]). Due to diffusion limitations the concentrations vary within the particle with the distance r to the particle centre. If the porous diameter is small compared with the particle radius, these distributions will be calculated using the homogenized form of the conservation equations given in Section 4, where local specific reaction rates per unit volume appear. These, in principle, should be obtained by multiplying the intrinsic combustion rates by the effective internal surface area of the pores per unit volume of the porous particle; although, as shown in Simons [16], there is a significant influence of the porous structure, mainly due to diffusion limitations in the small pores.

For the char oxidation we have considered a reduced mechanism including the three overall reactions 1, 2 and 3, of first order with respect to the local mean concentration of CO_2, O_2 and H_2O, measured by the product of the local gas density, ρ_g, and the mass fractions. We have considered the reactions to be of zero order with respect to the local char density, ρ_C. Obviously these three reaction rates must be equated to zero when the carbon of the particle is completely

consumed, and therefore a Heaviside function is also included as a factor. More precisely, the local homogenized reaction rates per unit volume within the particle are modelled using global Arrhenius laws of the form:

$$w_1 = B_1 e^{-E_1/\mathcal{R}T} \rho_g Y_{CO_2} H(\rho_C), \tag{3}$$

$$w_2 = B_2 e^{-E_2/\mathcal{R}T} \rho_g Y_{O_2} H(\rho_C), \tag{4}$$

$$w_3 = B_3 e^{-E_3/\mathcal{R}T} \rho_g Y_{H_2O} H(\rho_C), \tag{5}$$

where Y_{CO_2}, Y_{O_2} and Y_{H_2O} are the local mass fractions of CO_2, O_2 and H_2O in the gas filling the porous interstices, ρ_C is the partial density of fixed carbon in skeletal char particles and w_1, w_2 and w_3 correspond to the overall reactions 1, 2 and 3.

The char gasification rate, w_C, per unit volume

$$w_C = w_1 + w_2 + w_3 \tag{6}$$

is determined by the global rates of the reactions 1, 2 and 3.

The frequency factors B_1, B_2 and B_3, which are proportional to the internal pore surface per unit volume, will possibly grow when the local particle density, ρ_p, decreases below its initial value, ρ_p^0. However, for simplicity, we shall neglect these changes.

In addition to reactions 1–5 we shall take into account the following gas phase oxidation reactions:

- combustion of carbon monoxide:

$$\underline{6} \qquad CO + \frac{1}{2} O_2 \rightarrow CO_2 + (q_6);$$

- combustion of volatiles:

$$\underline{7} \qquad V_{(g)} + \nu_1 O_2 \rightarrow \nu_2 CO_2 + \nu_3 H_2O + \nu_4 SO_2 + (q_7);$$

- combustion of H_2:

$$\underline{8} \qquad H_2 + \frac{1}{2} O_2 \rightarrow H_2O + (q_8).$$

The molar stoichiometric coefficients ν_i are given by

$$\nu_1 = (2\kappa_1 + \kappa_2/2 + 2\kappa_4 - \kappa_3)/2, \qquad \nu_2 = \kappa_1,$$

$$\nu_3 = \kappa_2/2, \qquad \nu_4 = \kappa_4,$$

in terms of the composition of the volatile $V_{(g)} = C_{\kappa_1} H_{\kappa_2} O_{\kappa_3} S_{\kappa_4}$. As in our simplified model sulphur is only included in the volatiles, SO_2 is only produced by their oxidation with oxygen.

We shall allow for the reactions 6, 7 and 8 to occur either within the particle, or in a thin flame sheet surrounding the particle, or in the gas far away from the particles (see figure 1). The type of combustion that will occur will depend on the temperature and local concentrations of oxygen, carbon monoxide, volatiles and H_2 in the gas environment.

Accordingly we need to take into account two different cases. In the first case, when the particle lies in Ω_O, the volatiles, CO and H_2 produced by the gasification reactions are completely burnt, in a diffusion-controlled flame, inside the particle or outside in its vicinity. In this case the particles do not represent sources of CO, volatiles or H_2 for the mean values of the bulk interstitial gas.

In the second case, the homogeneous reactions 6, 7 and 8 do not take place in the particle or in its neighbourhood because there is no oxygen when they lie in Ω_F. Thus the volatiles, CO and H_2 join, without locally burning, the homogenized gas phase. As we shall see in

Section 3, if we assume combustion reactions 6, 7 and 8 to be infinitely fast, these species will burn, in the form of group combustion, when meeting the oxygen in a gaseous diffusion flame, corrugated by turbulence. This is the surface Γ_F in figure 1, separating a region Ω_F without oxygen from a region Ω_O where the volatiles, H_2 and CO are found only in the vicinity of the coal particles inside the surrounding flame sheets.

In the particular case of coal particles burning in the furnace of a power plant there are several inlets and several particle sizes given by the granulometric analysis of the coal. Thus, in the Lagrangian description of the particle evolution, we should distinguish several types of particles according to inlets and sizes. The combustion model follows the evolution of one single coal particle of each type through the boiler, evaluating the rate of mass and energy released at each point of the trajectory, in order to determine the sources in the gas phase model (see equations (8)–(16)).

3. Gas phase modelling

The coal particle combustion model to be developed in the next sections has to be coupled with a gas phase model to simulate the behaviour of a pulverized coal furnace. This gas phase model establishes the mean field, or local average conditions of the gas phase where the coal particles are burnt. They are represented by mean field values, denoted by the subscript or superscript g, of the mass fractions, temperature and velocity of the gaseous mixture.

Let $\mathcal{L}_g$ be the differential operator defined by

$$\mathcal{L}_g(u) = \frac{\partial(\rho_g u)}{\partial t} + \nabla \cdot (\rho_g u \mathbf{v}_g) - \nabla \cdot (\rho_g \mathcal{D} \nabla u), \tag{7}$$

where $\mathcal{D}$ is a gas phase diffusion coefficient which, for simplicity, although this is not a good assumption for H_2, will be considered to be the same for all species and equal to the thermal diffusivity. The extension of the Burke–Schumann analysis for diffusion controlled combustion in the gas phase, with non-unity Lewis numbers was developed for H_2/air combustion in Liñán *et al.* [17]. Then, the conservation equations of the gaseous species are given, see for instance Williams [18], by

$$\frac{\partial \rho_g}{\partial t} + \nabla \cdot (\rho_g \mathbf{v}_g) = f^{\mathrm{m}}, \tag{8}$$

$$\mathcal{L}_g(Y^g_{O_2}) = f^{\mathrm{m}}_{O_2} - \frac{4}{7} w_6 - \frac{32\nu_1}{M_{\mathrm{vol}}} w_7 - 8w_8, \tag{9}$$

$$\mathcal{L}_g(Y^g_{CO_2}) = f^{\mathrm{m}}_{CO_2} + \frac{11}{7} w_6 + \frac{44\nu_2}{M_{\mathrm{vol}}} w_7, \tag{10}$$

$$\mathcal{L}_g(Y^g_{H_2O}) = f^{\mathrm{m}}_{H_2O} + \frac{18\nu_3}{M_{\mathrm{vol}}} w_7 + 9w_8, \tag{11}$$

$$\mathcal{L}_g(Y^g_{SO_2}) = f^{\mathrm{m}}_{SO_2} + \frac{64\nu_4}{M_{\mathrm{vol}}} w_7, \tag{12}$$

$$\mathcal{L}_g(Y^g_{CO}) = f^{\mathrm{m}}_{CO} - w_6, \tag{13}$$

$$\mathcal{L}_g(Y^g_{V}) = f^{\mathrm{m}}_{V} - w_7, \tag{14}$$

$$\mathcal{L}_g(Y^g_{H_2}) = f^{\mathrm{m}}_{H_2} - w_8, \tag{15}$$

$$\mathcal{L}_g(h^g_{T}) = f^{\mathrm{e}} + q_6 w_6 + q_7 w_7 + q_8 w_8 - \nabla \cdot \mathbf{q}_{rg}, \tag{16}$$

where w_6, w_7 and w_8 denote, respectively, the mass consumption rates per unit volume of the volatiles, CO and H_2, due to the chemical reactions 6, 7 and 8, taking place in the gas phase; h_T^g is the gas phase specific thermal enthalpy, which we shall for simplicity write as $c_p T^g$ considering the gas phase specific heat at constant pressure, c_p, to be constant, and $\mathbf{q}_{rg}$ is the radiant heat flux vector.

We have included the effect of the particles as homogenized sources in the gas phase denoted by f^m, f^e and f_α^m, $\alpha = O_2, CO_2, H_2O, SO_2, CO, V, H_2$ (which is justified because of the small volumetric fraction of the particles compared with that of the gas). These sources will be calculated later after analysing the distribution of temperature and concentrations within the individual particles and in the gaseous neighbourhood of each particle.

The equations should be complemented with the momentum conservation equations. In the turbulent flow in the furnace, these equations apply to the fluctuating variables. One must use modelling assumptions to derive from them the equations describing the local average values.

For the gas phase reaction rates we could adopt overall expressions of the form

$$w_6 = \rho_g^2 Y_{O_2}^{1/2} Y_{CO} Y_{H_2O}^{1/2} B_6 e^{-E_6/\mathcal{R}T}, \tag{17}$$

$$w_7 = \rho_g^{1+\nu_1} Y_{O_2}^{\nu_1} Y_V B_7 e^{-E_7/\mathcal{R}T}, \tag{18}$$

$$w_8 = \rho_g^{3/2} Y_{O_2}^{1/2} Y_{H_2} B_8 e^{-E_8/\mathcal{R}T}, \tag{19}$$

where the factor $Y_{H_2O}^{1/2}$ accounts for the fact that reaction 6 is catalysed by water vapour. However in our analysis we shall consider that the limit of infinite reaction rates applies, leading to the non-coexistence of CO, V and H_2 with O_2, independently of the detailed form of the rates.

In order to obtain equations without the gas phase reaction terms we consider the following conserved scalars or linear combinations of Shvab–Zeldovich type:

$$\beta_1^g = Y_{O_2}^g - \frac{4}{7} Y_{CO}^g - \frac{32\nu_1}{M_{vol}} Y_V^g - 8 Y_{H_2}^g, \tag{20}$$

$$\beta_2^g = Y_{CO_2}^g + \frac{11}{7} Y_{CO}^g + \frac{44\nu_2}{M_{vol}} Y_V^g, \tag{21}$$

$$\beta_3^g = Y_{H_2O}^g + \frac{18\nu_3}{M_{vol}} Y_V^g + 9 Y_{H_2}^g, \tag{22}$$

$$\beta_4^g = Y_{SO_2}^g + \frac{64\nu_4}{M_{vol}} Y_V^g, \tag{23}$$

$$H^g = h_T^g + q_6 Y_{CO}^g + q_7 Y_V^g + q_8 Y_{H_2}^g. \tag{24}$$

In more simplified descriptions of the diffusion controlled gas phase oxidation of the volatiles and CO a single mixture fraction – a normalized form of the coupling function – was used by Smith *et al.* [12]; while two mixture fractions were introduced by Flores and Fletcher [19]. The non-proportionality of the distributed sources forces us to introduce the five coupling functions: the first relates the oxygen and the reactants, and the remaining determine the products and the thermal energy. Then from equations (9)–(16) we have

$$\mathcal{L}_g(\beta_1^g) = f_{O_2}^m - \frac{4}{7} f_{CO}^m - \frac{32\nu_1}{M_{vol}} f_V^m - 8 f_{H_2}^m, \tag{25}$$

$$\mathcal{L}_g(\beta_2^g) = f_{CO_2}^m + \frac{11}{7} f_{CO}^m + \frac{44\nu_2}{M_{vol}} f_V^m, \tag{26}$$

$$\mathcal{L}_g(\beta_3^g) = f_{H_2O}^m + \frac{18\nu_3}{M_{vol}} f_V^m + 9 f_{H_2}^m, \tag{27}$$

$$\mathcal{L}_g(\beta_4^g) = f_{SO_2}^m + \frac{64\nu_4}{M_{vol}} f_V^m, \tag{28}$$

$$\mathcal{L}_g(H^g) = f^e + q_6 f_{CO}^m + q_7 f_V^m + q_8 f_{H_2}^m - \nabla \cdot \mathbf{q}_{rg}, \tag{29}$$

which must be complemented with a description of the sources.

If, following the Burke–Schumann analysis, we assume that the gas phase reactions 6, 7 and 8 are infinitely fast, oxygen cannot coexist with the volatiles, H_2 and CO. The reactions 6, 7 and 8 take place in an infinitely thin flame sheet, whose location is given by $\beta_1^g = 0$, with w_6, w_7 and w_8 acting as Dirac delta functions. In the region Ω_F, defined by $\beta_1^g \leq 0$, the mass fraction $Y_{O_2}^g$ is zero so the particles are gasifying in an oxygen free environment and $w_6 = w_7 = w_8 = 0$. In that region the local values of H^g, β_1^g, β_2^g, β_3^g and β_4^g determine the thermal enthalpy and all mass fractions $Y_{CO_2}^g$, $Y_{H_2O}^g$ and $Y_{SO_2}^g$ in terms of Y_{CO}^g, Y_V^g and $Y_{H_2}^g$.

In order to calculate Y_V^g, $Y_{H_2}^g$ and Y_{CO}^g in this region, (25) for β_1^g has to be supplemented with two of the conservation equations for Y_V^g, $Y_{H_2}^g$ or Y_{CO}^g. For example with equations

$$\mathcal{L}_g(Y_V^g) = f_V^m \quad \text{in } \Omega_F, \tag{30}$$

$$\mathcal{L}_g(Y_{H_2}^g) = f_{H_2}^m \quad \text{in } \Omega_F, \tag{31}$$

which must be integrated using the boundary conditions $Y_V^g = 0$ and $Y_{H_2}^g = 0$ on the surface Γ_F, given by $\beta_1^g = 0$, which separates the domains Ω_O and Ω_F where $\beta_1^g > 0$ and $\beta_1^g < 0$, respectively. Then, the mass fraction Y_{CO}^g is obtained from (20). Notice that Y_{CO}^g, Y_V^g and $Y_{H_2}^g$ are not proportional to each other because typically f_V^m, $f_{H_2}^m$ and f_{CO}^m are not in a constant ratio.

In the region Ω_O we find oxygen in the gaseous environment of the particles. Then the volatiles, H_2 and CO generated by the gasification will react with this oxygen in a diffusion flame sheet (the boldface circles in figure 1). This, as we shall see in Sections 4 and 5, may be either inside or outside the particle depending on the local mean field values of the temperature and species concentration in the ambient gas.

In Ω_O, where $Y_{CO}^g = Y_V^g = Y_{H_2}^g = 0$, we have

$$Y_{O_2}^g = \beta_1^g, \quad Y_{CO_2}^g = \beta_2^g, \quad Y_{H_2O}^g = \beta_3^g, \quad Y_{SO_2}^g = \beta_4^g, \quad h_T^g = H^g. \tag{32}$$

To calculate the source terms in the equations for the β_i^g and H^g, namely f_α^m and f^e, we need to describe the response of the particle and the details of the gas in its vicinity, accounting for the effect of the oxidation reactions of the volatiles, CO and H_2. This analysis will be carried out in Section 4 to describe the distribution inside the particle, $r < a$, and in Section 5 for the gas phase response in the neighbourhood, $a < r \ll l_p$, outside the particle.

The condition for the model used in this paper of gas phase diffusion controlled combustion in flame sheets is based on the requirement that the value of the Damköhler number – or ratio of the diffusion and chemical times – is large compared to unity. For combustion in a flame sheet surrounding the particle the diffusion time to be used is the square of the particle radius (or better of the flame sheet radius) divided by the mass diffusivity, evaluated at the flame temperature. However, the conditions for group diffusion controlled combustion are not so strict, because the corresponding Damköhler number is based on the typically much larger diffusion times associated with the scales of the gas phase turbulent flow.

4. Modelling the particle gasification

We shall deal with coal particles that contain a significant fraction of ashes not lost during the devolatilization or char oxidation stages. Thus we shall consider in our model that the apparent radius of each particle remains constant, although the density of H_2O, volatiles and char will change with time. We shall model the devolatilization as a spatially uniform volumetric pyrolysis reaction, because the temperature will be considered to be nearly uniform within the small particles.

The reader should notice that the details of the model for the moisture evaporation, generation of combustible volatiles and char oxidation by O_2, CO_2 and H_2O, to be given in this section, are not essential for the validity of the gas phase description that has been given above. Indeed this gas phase description is valid for more general models of devolatilization and char oxidation processes, which are simpler to describe for coals with low ash content.

As mentioned above, we shall assume that during devolatilization and char oxidation the porous particle retains its initial diameter and maintains a constant density of ashes ρ_{ash}. This density as well as the initial densities of water, volatiles and char are given by a proximate analysis of the coal. More precisely, the density of the coal particle is given by

$$\rho_p = \rho_{H_2O} + \rho_V + \rho_C + \rho_{\text{ash}}. \tag{33}$$

The evolution of ρ_{H_2O}, ρ_V and ρ_C, with the radial coordinate r and time t, will be given by

$$\frac{\partial \rho_V}{\partial t} = -w_4, \qquad \frac{\partial \rho_{H_2O}}{\partial t} = -w_5, \qquad \frac{\partial \rho_C}{\partial t} = -w_C, \tag{34}$$

in terms of the mass rates, per unit volume and time, of generation of volatiles w_4, water vapour w_5 and char gasification w_C, given by equations (1)–(6).

If, for simplicity in the presentation, we restrict our attention to the case of low Peclet number, based on the relative velocity of the particle to the local gas environment, then the effects of the motion of this ambient gas relative to the particle may be neglected, so that the concentration and temperature fields within the particle and in its neighbourhood may be considered spherico-symmetrical. For the more complicated case of higher Peclet numbers, corrector factors should be introduced in the gas phase sources from the particle.

When we analyse the gas phase inside the particle, $r < a$, let ρ_g be the density of the gas in the porous region, and let v_g be the effective radial velocity of the gas, defined so that $\rho_g v_g$ is the radial gas mass flux, per unit surface. Then the mass conservation equation for the gas phase can be written as

$$\frac{1}{r^2}\frac{\partial}{\partial r}(r^2 \rho_g v_g) = w_4 + w_5 + w_C, \tag{35}$$

where, because $\rho_g \ll \rho_p$, we have neglected the time derivative term representing the gas accumulation within the pores.

We shall also write the mass conservation equations

$$\mathcal{L}_c(Y_{O_2}) = -\frac{4}{3}w_2 - \frac{4}{7}w_6 - \frac{32\nu_1}{M_{\text{vol}}}w_7 - 8w_8, \tag{36}$$

$$\mathcal{L}_c(Y_{CO_2}) = -\frac{11}{3}w_1 + \frac{11}{7}w_6 + \frac{44\nu_2}{M_{\text{vol}}}w_7, \tag{37}$$

$$\mathcal{L}_c(Y_{H_2O}) = -\frac{3}{2}w_3 + w_5 + \frac{18\nu_3}{M_{\text{vol}}}w_7 + 9w_8, \tag{38}$$

$$\mathcal{L}_c(Y_{SO_2}) = \frac{64\nu_4}{M_{\text{vol}}}w_7, \tag{39}$$

$$\mathcal{L}_c(Y_{CO}) = \frac{14}{3}w_1 + \frac{7}{3}w_2 + \frac{7}{3}w_3 - w_6, \tag{40}$$

$$\mathcal{L}_c(Y_V) = w_4 - w_7, \tag{41}$$

$$\mathcal{L}_c(Y_{H_2}) = \frac{1}{6}w_3 - w_8, \tag{42}$$

describing the evolution of mass fractions in the gas phase within the pores of the particles. Here $\mathcal{L}_c$ is the differential operator, written in spherical coordinates,

$$\mathcal{L}_c(u) = \frac{1}{r^2}\frac{\partial}{\partial r}(r^2\rho_g v_g u) - \frac{1}{r^2}\frac{\partial}{\partial r}\left(r^2\rho_g \mathcal{D}_e \frac{\partial u}{\partial r}\right), \tag{43}$$

similar to the stationary form of operator $\mathcal{L}_g$ defined in (7).

In these equations we have neglected again the time derivative terms, and we shall represent the diffusive fluxes by the Fick's law with an effective diffusion coefficient through the porous particle, $\mathcal{D}_e$, equal for all the gaseous species. The density ρ_g appearing in these equations is related to local temperature T and pressure p by the equation of state for a mixture of perfect gases

$$p = \rho_g T\mathcal{R}/M, \tag{44}$$

where $\mathcal{R}$ is the universal gas constant and M is the molecular mass of the gas mixture.

The spatial pressure variations within the particle, given by Darcy's law, will be neglected compared with the ambient gas pressure, i.e. $p = p_g$; then, the momentum equation will not be written here.

Even though the effective diffusivity changes with porosity, and thereby with the solid density, we shall neglect these changes considering it to be constant.

As boundary conditions for equations (35)–(42) we must impose the symmetry conditions

$$v_g = \frac{\partial Y_\alpha}{\partial r} = 0 \quad \text{at } r = 0, \quad \text{for } \alpha = O_2, CO_2, H_2O, SO_2, CO, V, H_2, \tag{45}$$

and also the continuity of the values of the mass fractions with those in the gas phase adjacent to the particle surface. In addition, we must add the equations of mass conservation at the interface. The values of the temperature T_p and the mass fractions Y_α^s, at $r = a$ (the radius of the particle) can only be calculated by analysing the gas phase in the neighbourhood of the particle.

When writing the energy equation, we shall take into account that the gasification time is long compared with the heat conduction time, $a^2\rho_p^0 c_s/k_e$, based on the effective conductivity k_e and the specific heat c_s of the solid phase which, for simplicity in the presentation, are considered to be constant. If this is the case we can neglect the spatial variations of the temperature T within the particle and, then, write $T = T_p(t)$. The assumption of uniformity of the temperature within the particle is based on the criterium that the heat conduction time across the particle is short compared with the corresponding diffusion time. Then, the reactions within the particle will generate temperature variations (which in the case of diffusion controlled gas phase reactions will lead to peaks) that are small compared with the temperature itself. This temperature is given by the integrated form of the energy equation,

$$\frac{4}{3}\pi a^3 \rho_p c_s \frac{dT_p}{dt} = 4\pi a^2(q_p'' + q_r'') + \int_0^a \left(\sum_{i=1}^{8} q_i w_i\right) 4\pi r^2 dr, \tag{46}$$

where $4\pi a^2 q_p''$ and $4\pi a^2 q_r''$ are the rate of heat reaching the particle by conduction and radiation. They are given by

$$q_p'' = k\frac{dT}{dr}_{|_{r=a^+}}, \quad q_r'' = \varepsilon_p \left(\frac{1}{4} \int_{S^2} I(x, \omega) d\omega - \sigma T_p^4 \right), \tag{47}$$

where $I(x, \omega)$ is the radiation intensity in the direction ω at the position of the particle, denoted by x, ε_p is the particle emissivity and S^2 is the unit sphere.

From the approximation $T = T_p(t)$ within the particle, and the laws given by equations (1)–(2), the rates of generation of water vapour and volatiles per particle are uniform within the particle and known functions of T_p, allowing us to calculate the change with time of the condensed phase values of ρ_V and ρ_{H_2O}:

$$\frac{d\rho_V}{dt} = -w_4(T_p) = -B_4 e^{-E_4/\mathcal{R}T_p} \rho_V, \tag{48}$$

$$\frac{d\rho_{H_2O}}{dt} = -w_5(T_p) = -B_5 e^{-E_5/\mathcal{R}T_p} \rho_{H_2O}, \tag{49}$$

resulting also in a contribution of w_4 and w_5 to the energy equation (46), given by $\frac{4}{3}\pi a^3 (w_4 q_4 + w_5 q_5)$.

While w_4 and w_5 are spatially uniform and known functions of T_p, the dependence of w_1, w_2 and w_3 on Y_{CO_2}, Y_{O_2} and Y_{H_2O}, which, due to internal diffusion limitations, are not uniform within the particle, makes it more difficult the solution of the third equation in (34). Indeed, in order to calculate ρ_C, the values of Y_{O_2}, Y_{CO_2} and Y_{H_2O} within the particle have to be calculated by solving equations (36)–(42) for given values of T_p and of the mass fractions at the particle surface.

The solution of this problem should be carried out numerically following the Lagrangian history of the coal particle in its time evolving environment. This environment determines the heat fluxes (47) as well as the mass fractions $Y^s_{CO_2}$, $Y^s_{O_2}$ and $Y^s_{H_2O}$ on the surface of the particle, which can only be obtained after analysing, in Section 5, the gas phase response in the neighbourhood of the particle.

If the particle lies in Ω_F, or in Ω_O with $\beta_1^s < 0$, there is no oxygen inside the particle and the gas phase reactions terms w_6, w_7 and w_8 disappear from equations (36)–(42). The corresponding analysis, which is given later in this section, simplifies considerably.

However to analyse the case where $\beta_1^s > 0$, when the oxygen reaches the particle surface, is more complicated and it will be done using the assumption that the oxidation reaction times are infinitely small compared with the diffusion times within the particles. This implies that there is a diffusion controlled flame inside the particle at $r = r_f < a$.

Let us first consider the case, $\beta_1^s > 0$, with a diffusion controlled flame inside the particle, i.e., $r_f < a$. In order to eliminate the source terms associated with reactions 6, 7 and 8, to facilitate the analysis when their rates can be considered infinitely fast, we introduce the following Schvab–Zeldovich coupling functions

$$\beta_1 = Y_{O_2} - \frac{4}{7} Y_{CO} - \frac{32\nu_1}{M_{vol}} Y_V - 8Y_{H_2}, \tag{50}$$

$$\beta_2 = Y_{CO_2} + \frac{11}{7} Y_{CO} + \frac{44\nu_2}{M_{vol}} Y_V, \tag{51}$$

$$\beta_3 = Y_{H_2O} + \frac{18\nu_3}{M_{vol}} Y_V + 9Y_{H_2}, \tag{52}$$

$$\beta_4 = Y_{SO_2} + \frac{64\nu_4}{M_{vol}} Y_V, \tag{53}$$

which satisfy the conservation equations

$$\mathcal{L}_c(\beta_1) = -\frac{8}{3}(w_1 + w_2 + w_3) - \frac{32\nu_1}{M_{\text{vol}}}w_4, \tag{54}$$

$$\mathcal{L}_c(\beta_2) = \frac{11}{3}(w_1 + w_2 + w_3) + \frac{44\nu_2}{M_{\text{vol}}}w_4, \tag{55}$$

$$\mathcal{L}_c(\beta_3) = w_5 + \frac{18\nu_3}{M_{\text{vol}}}w_4, \tag{56}$$

$$\mathcal{L}_c(\beta_4) = \frac{64\nu_4}{M_{\text{vol}}}w_4. \tag{57}$$

Notice that (50)–(53) correspond to the same Schvab–Zeldovich combinations defined in (20)–(23), although now the superscript g is omitted here and in the following sections, to point out that we are not considering the mean field values but the local gas phase values. In the limit of infinitely fast gas phase reactions 6, 7 and 8 we are considering, we must complement the system of conservation equations (54)–(57) with the Burke–Schumann condition that oxygen cannot coexist with the gaseous volatiles, H_2 and CO. All are consumed at a flame sheet inside the particle, at $r = r_f$ where $\beta_1 = 0$, separating an interior region, $\beta_1 < 0$, without oxygen, from an exterior region, $\beta_1 > 0$, where there are no volatiles, H_2 or CO. Notice that the volatiles produced in the region $\beta_1 > 0$ are locally consumed immediately after gasification.

As indicated before the validity of the Burke–Schumann description of the effect of gas phase reactions inside the particle is conditioned to having values of the Damköhler numbers, or ratio of the diffusion time $a^2/\mathcal{D}_e$ and the reaction times, large compared with unity. In this case the reaction is confined to a thin layer, of thickness δ_r small compared with the particle radius a, the ratio δ_r/a growing only to values of order unity when the Damköhler number decreases to values of order unity. For large Damköhler numbers the reaction term behaves as a Dirac delta source, located in the flame sheet, with the appropriate value to ensure that outside the mass fraction of the volatiles, CO and H_2 are small. Due to the assumed large value of the heat conductivity the temperature distribution does not exhibit a peak in the flame sheet.

We notice that equations (54)–(57) are still difficult to solve. Instead, in order to develop a simplified treatment of the effects of the gasification char reactions 1, 2 and 3, we shall take into account that the overall activation energies of these reactions are large. Then, Damköhler numbers, which can be defined for these reactions as the ratio of the characteristic values of the diffusion term and the reaction term in the conservation equations (36)–(38) for O_2, CO_2 and H_2O, i.e.,

$$\text{Da}_i = (a^2/\mathcal{D}_e)B_i e^{-E_i/\mathcal{R}T_p}, \quad i = 1, 2, 3, \tag{58}$$

are strongly temperature dependent. More precisely, we consider that the activation energies of reactions 1, 2 and 3 are large enough, so that the transition stage when Da_1, Da_2 or Da_3 are of order unity is short. Then reactions 1, 2 and 3 will be consider either frozen, when the Damköhler numbers are smaller than 1, or very fast when they are much larger than 1. At low T_p, the values of Da_1, Da_2 and Da_3 are small so the char oxidation reactions can be neglected in first approximation, because they give contributions to w_1, w_2 and w_3 (and also to the energy equation) negligible when compared with w_4 and w_5, while the energy reaching the particle by conduction is comparable with the energy needed for occurrence of reactions 4 and 5.

Thus, when $\text{Da}_i \ll 1$, $i = 1, 2, 3$, there is no production of CO or H_2 within the particle, and we can simplify (35) by writing $w_C = 0$ and the conservation equations (36)–(42) by writing $w_1 = w_2 = w_3 = w_6 = w_8 = 0$. If, in addition, we assume that the gas phase reaction

7, between the volatiles and oxygen, is infinitely fast we can further simplify the analysis, according to the value

$$\beta_1^s = Y_{O_2}^s - \frac{32\nu_1}{M_{vol}} Y_V^s,$$

of β_1 at the particle surface:

For $\beta_1^s < 0$ there is a diffusion flame outside the particle that prevents the oxygen to reach the surface. In this case the energy equation for the evolution of T_p simplifies to

$$\frac{4}{3}\pi a^3 \rho_p c_s \frac{dT_p}{dt} = 4\pi a^2 (q_p'' + q_r'') + \frac{4}{3}\pi a^3 (q_4 w_4 + q_5 w_5). \tag{59}$$

For $\beta_1^s > 0$, the volatiles are prevented from leaving the particle by the fast reaction with the oxygen. In this case the energy equation becomes

$$\frac{4}{3}\pi a^3 \rho_p c_s \frac{dT_p}{dt} = 4\pi a^2 (q_p'' + q_r'') + \frac{4}{3}\pi a^3 \{(q_4 + q_7) w_4 + q_5 w_5\}. \tag{60}$$

In order to complete the description of the evolution of ρ_V, ρ_{H_2O} and T_p we need to calculate not only q_r'' but also q_p'', which results from the analysis of the gaseous neighbourhood of the particle, to be given in Section 5.

At high particle temperatures, the opposite limit of large Damköhler numbers ($Da_i \gg 1$, $i = 1, 2, 3$) is applicable. The char and CO_2, O_2 and H_2O cannot coexist, and the reactions become diffusion controlled. The reaction terms w_1, w_2 and w_3 in (35) and (54)–(55) become Dirac delta sources at some $r = r_c(t)$, with strengths m_1'', m_2'' and m_3'' determined so as to ensure that $Y_{CO_2} = Y_{O_2} = Y_{H_2O} = 0$ at $r \le r_c$ and $\rho_C = 0$ at $r > r_c$ (only ashes are present in the particle for r in the interval $(r_c, a]$). Thus, in this limit case, we are led to the shrinking core model, see Bhatia [20] (see figure 2).

If we anticipate that $r_f > r_c$ so that $\beta_1(r_c) < 0$, then there is no oxygen where the char gasification occurs, and therefore $w_2 = 0$ and the contributions of reactions 1, 2 and 3 to the energy equation reduce to $4\pi r_c^2 (m_1'' q_1 + m_3'' q_3)$.

At this shrinking core stage, equations (35) and (54)–(56) can be integrated once to give

$$r^2 \rho_g v_g = (w_4 + w_5) r^3/3 + (m_1'' + m_3'') r_c^2, \tag{61}$$

$$r^2 \rho_g v_g \beta_1 - r^2 \rho_g \mathcal{D}_e \frac{\partial \beta_1}{\partial r} = -\frac{8}{3}(m_1'' + m_3'') r_c^2 - \frac{32\nu_1}{M_{vol}} w_4 \frac{r^3}{3}, \tag{62}$$

$$r^2 \rho_g v_g \beta_2 - r^2 \rho_g \mathcal{D}_e \frac{\partial \beta_2}{\partial r} = \frac{11}{3}(m_1'' + m_3'') r_c^2 + \frac{44\nu_2}{M_{vol}} w_4 \frac{r^3}{3}, \tag{63}$$

$$r^2 \rho_g v_g \beta_3 - r^2 \rho_g \mathcal{D}_e \frac{\partial \beta_3}{\partial r} = \left(w_5 + \frac{18\nu_3}{M_{vol}} w_4 \right) \frac{r^3}{3}, \tag{64}$$

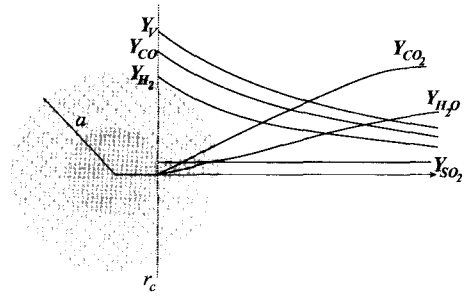

Figure 2. Shrinking core.

for $r > r_c$, and

$$r^2 \rho_g v_g = (w_4 + w_5) r^3/3, \tag{65}$$

$$Y_{CO_2} = Y_{O_2} = Y_{H_2O} = 0, \tag{66}$$

for $r \leq r_c$.

The solution of the system of equations (61)–(64) with the boundary conditions

$$Y_{CO} = Y_V = Y_{H_2} = 0 \quad \text{at } r = a, \tag{67}$$

$$Y_{O_2} = Y_{CO} = Y_V = Y_{H_2} = 0 \quad \text{at } r = r_f, \tag{68}$$

$$Y_{CO_2} = Y_{O_2} = Y_{H_2O} = 0 \quad \text{at } r = r_c \tag{69}$$

will be written explicitly here, based on the reasonable assumption that during the early phases of the char combustion stage, when the reactions 4 and 5 are not yet negligible, we can approximate in (61) the factor $r^3/3$ by $a^3/3$, because $a - r_c \ll a$.

The total mass gasification reaction rate is $4\pi \dot{m}$, where $\dot{m}$, which is the value of $\rho_g v_g r^2$ evaluated at $r = a$, includes the contributions $\dot{m}_i$, of reactions 1, 3, 4 and 5,

$$\dot{m} = (m_1'' + m_3'') r_c^2 + (w_4 + w_5) a^3/3. \tag{70}$$

Equations (62)–(64), with $r^2 \rho_g v_g$ replaced by $\dot{m}$ will be integrated now with the assumption that $\rho_g \mathcal{D}_e$ does not vary with r. The solution, in $r_c \leq r \leq a$, will be written in terms of the nondimensional gasification rate and the nondimensional rate for reaction i, respectively defined by

$$\lambda = \frac{\dot{m}}{\rho_g a \mathcal{D}}, \quad \lambda_i = \frac{\dot{m}_i}{\rho_g a \mathcal{D}}, \quad i = 1, 3, 4, 5. \tag{71}$$

Then $\lambda = \lambda_1 + \lambda_3 + \lambda_4 + \lambda_5$ and

$$\beta_1 = -\frac{8}{3}\left(\frac{\lambda_1}{\lambda} + \frac{\lambda_3}{\lambda}\right) - \frac{32\nu_1}{M_{vol}}\frac{\lambda_4}{\lambda} + \left\{Y_{O_2}^s + \frac{8}{3}\left(\frac{\lambda_1}{\lambda} + \frac{\lambda_3}{\lambda}\right) + \frac{32\nu_1}{M_{vol}}\frac{\lambda_4}{\lambda}\right\} e^{\lambda \frac{\mathcal{D}}{\mathcal{D}_e}(1 - a/r)}, \tag{72}$$

$$\beta_2 = \frac{11}{3}\left(\frac{\lambda_1}{\lambda} + \frac{\lambda_3}{\lambda}\right) + \frac{44\nu_2}{M_{vol}}\frac{\lambda_4}{\lambda} + \left\{Y_{CO_2}^s - \frac{11}{3}\left(\frac{\lambda_1}{\lambda} + \frac{\lambda_3}{\lambda}\right) - \frac{44\nu_2}{M_{vol}}\frac{\lambda_4}{\lambda}\right\} e^{\lambda \frac{\mathcal{D}}{\mathcal{D}_e}(1 - a/r)}, \tag{73}$$

$$\beta_3 = \frac{\lambda_5}{\lambda} + \frac{18\nu_3}{M_{vol}}\frac{\lambda_4}{\lambda} + \left\{Y_{H_2O}^s - \frac{\lambda_5}{\lambda} - \frac{18\nu_3}{M_{vol}}\frac{\lambda_4}{\lambda}\right\} e^{\lambda \frac{\mathcal{D}}{\mathcal{D}_e}(1 - a/r)}, \tag{74}$$

where $Y_{O_2}^s$, $Y_{CO_2}^s$ and $Y_{H_2O}^s$ are the surface values of Y_{O_2}, Y_{CO_2} and Y_{H_2O} to be calculated later on from the gas phase analysis.

The flame position, $r = r_f$, is obtained with the requirement that $\beta_1(r_f) = 0$, leading to

$$\frac{8}{3}\left(\frac{\lambda_1}{\lambda} + \frac{\lambda_3}{\lambda}\right) + \frac{32\nu_1}{M_{vol}}\frac{\lambda_4}{\lambda} = \left\{Y_{O_2}^s + \frac{8}{3}\left(\frac{\lambda_1}{\lambda} + \frac{\lambda_3}{\lambda}\right) + \frac{32\nu_1}{M_{vol}}\frac{\lambda_4}{\lambda}\right\} e^{\lambda \frac{\mathcal{D}}{\mathcal{D}_e}(1 - a/r_f)}, \tag{75}$$

while the use of conditions $Y_{CO_2} = Y_{O_2} = Y_{H_2O} = 0$ at $r = r_c$ in equations (73)–(74) together with (51) and (52) lead to

$$\frac{11}{7} Y_{CO}^c + \frac{44\nu_2}{M_{vol}} Y_V^c = \frac{11}{3}\left(\frac{\lambda_1}{\lambda} + \frac{\lambda_3}{\lambda}\right) + \frac{44\nu_2}{M_{vol}}\frac{\lambda_4}{\lambda} + \left\{Y_{CO_2}^s - \frac{11}{3}\left(\frac{\lambda_1}{\lambda} + \frac{\lambda_3}{\lambda}\right) - \frac{44\nu_2}{M_{vol}}\frac{\lambda_4}{\lambda}\right\} e^{\lambda \frac{\mathcal{D}}{\mathcal{D}_e}(1 - a/r_c)}, \tag{76}$$

$$\frac{18\nu_3}{M_{vol}} Y_V^c + 9 Y_{H_2}^c = \frac{\lambda_5}{\lambda} + \frac{18\nu_3}{M_{vol}}\frac{\lambda_4}{\lambda} + \left\{Y_{H_2O}^s - \frac{\lambda_5}{\lambda} - \frac{18\nu_3}{M_{vol}}\frac{\lambda_4}{\lambda}\right\} e^{\lambda \frac{\mathcal{D}}{\mathcal{D}_e}(1 - a/r_c)}. \tag{77}$$

In order to obtain Y^c_{CO}, $Y^c_{H_2}$ and Y^c_V, we must integrate the three mass conservation equations for CO, V and H_2 with the corresponding boundary conditions given by equation (68), resulting in

$$Y^c_{CO} = \left(\frac{14}{3}\frac{\lambda_1}{\lambda} + \frac{7}{3}\frac{\lambda_3}{\lambda}\right)\left\{1 - e^{\lambda\frac{\mathcal{D}}{\mathcal{D}_e}\left(\frac{a}{r_f}-\frac{a}{r_c}\right)}\right\}, \tag{78}$$

$$Y^c_{H_2} = \frac{1}{6}\frac{\lambda_3}{\lambda}\left\{1 - e^{\lambda\frac{\mathcal{D}}{\mathcal{D}_e}\left(\frac{a}{r_f}-\frac{a}{r_c}\right)}\right\}, \tag{79}$$

$$Y^c_V = \frac{\lambda_4}{\lambda}\left\{1 - e^{\lambda\frac{\mathcal{D}}{\mathcal{D}_e}\left(\frac{a}{r_f}-\frac{a}{r_c}\right)}\right\}. \tag{80}$$

Finally, we use (34) to determine the time evolution of r_c. If we neglect the changes in ρ_C within the char core, during the first stage of the kinetically controlled char gasification, we can approximate ρ_C by its initial value ρ^0_C for $r < r_c$, and then we obtain

$$\frac{\rho^0_C}{\rho_g a\mathcal{D}} r_c^2 \frac{dr_c}{dt} = -(\lambda_1 + \lambda_3). \tag{81}$$

We can now evaluate the contributions of w_1, w_3, w_6, w_7 and w_8 to the energy equation as

$$4\pi\rho_g a\mathcal{D}\left\{\lambda_1(q_1 + 14q_6/3) + \lambda_3(q_3 + 7q_6/3 + q_8/6) + \lambda_4 q_7\right\}. \tag{82}$$

Let us now consider the cases where the flame lies outside the particle, preventing the oxygen to approach the particle surface. In these cases, the mass conservation equations describing the radial distribution of the gas phase mass fractions Y_{CO_2} and Y_{H_2O}, within the pores of the particles, are (37) and (38) with $w_6 = w_7 = w_8 = 0$. These equations can be integrated once, in the limit of $Da_i \gg 1$, for $i = 1, 3$, to give

$$r^2\rho_g v_g Y_{CO_2} - r^2\rho_g\mathcal{D}_e\frac{\partial Y_{CO_2}}{\partial r} = -\frac{11}{3}m''_1 r_c^2, \tag{83}$$

$$r^2\rho_g v_g Y_{H_2O} - r^2\rho_g\mathcal{D}_e\frac{\partial Y_{H_2O}}{\partial r} = -\frac{3}{2}m''_3 r_c^2 + w_5\frac{r^3}{3}, \tag{84}$$

for $r_c < r < a$, with the boundary conditions

$$Y_{CO_2} = Y_{H_2O} = 0 \quad \text{at } r = r_c, \tag{85}$$

leading to

$$\frac{11}{3}\frac{\lambda_1}{\lambda} = \left\{Y^s_{CO_2} + \frac{11}{3}\frac{\lambda_1}{\lambda}\right\}e^{\lambda\frac{\mathcal{D}}{\mathcal{D}_e}\left(1-\frac{a}{r_c}\right)}, \tag{86}$$

$$\frac{3}{2}\frac{\lambda_3}{\lambda} - \frac{\lambda_5}{\lambda} = \left\{Y^s_{H_2O} + \frac{3}{2}\frac{\lambda_3}{\lambda} - \frac{\lambda_5}{\lambda}\right\}e^{\lambda\frac{\mathcal{D}}{\mathcal{D}_e}\left(1-\frac{a}{r_c}\right)}, \tag{87}$$

where we recall that $Y^s_{CO_2}$ and $Y^s_{H_2O}$ are the surface values of Y_{CO_2} and Y_{H_2O} to be calculated using the gas phase analysis.

Finally, the time evolution of r_c is determined by (81), whereas the contributions of w_1 and w_3 to the energy equation can be evaluated as

$$4\pi\rho_g a\mathcal{D}\left(\lambda_1 q_1 + \lambda_3 q_3\right). \tag{88}$$

In summary, in the first stage, when, because Da_1, Da_2 and Da_3 are $\ll 1$, the char oxidation reactions are kinetically controlled, we have

$$\frac{d\rho_C}{dt} = -\frac{3\rho_g\mathcal{D}}{a^2}(\lambda_1 + \lambda_2 + \lambda_3), \tag{89}$$

$$\frac{d\rho_V}{dt} = -\frac{3\rho_g \mathcal{D}}{a^2}\lambda_4, \tag{90}$$

$$\frac{d\rho_{H_2O}}{dt} = -\frac{3\rho_g \mathcal{D}}{a^2}\lambda_5, \tag{91}$$

where the nondimensional reaction rates λ_i are given by

$$\lambda_1 = \frac{a^2}{3\mathcal{D}} B_1 e^{-E_1/\mathcal{R}T_p} Y^s_{CO_2} H(\rho_C), \tag{92}$$

$$\lambda_2 = \frac{a^2}{3\mathcal{D}} B_2 e^{-E_2/\mathcal{R}T_p} Y^s_{O_2} H(\rho_C), \tag{93}$$

$$\lambda_3 = \frac{a^2}{3\mathcal{D}} B_3 e^{-E_3/\mathcal{R}T_p} Y^s_{H_2O} H(\rho_C), \tag{94}$$

$$\lambda_4 = \frac{a^2}{3\rho_g \mathcal{D}} B_4 e^{-E_4/\mathcal{R}T_p} \rho_V, \tag{95}$$

$$\lambda_5 = \frac{a^2}{3\rho_g \mathcal{D}} B_5 e^{-E_5/\mathcal{R}T_p} \rho_{H_2O}, \tag{96}$$

although, with good approximation, λ_1, λ_2 and λ_3 can be written equal to zero.

In the second stage, when any $\mathrm{Da}_i \gg 1$, $i = 1, 2, 3$, we shall still use equations (90)–(91) and (95)–(96), but replace equations (89) by (81) and (92)–(94) by (75)–(80) and $\lambda_2 = 0$, when $r_f < a$, and by (86)–(87) and $\lambda_2 = 0$, when $r_f > a$ or there is no oxygen in the vicinity of the particle .

In both cases, in order to get a closed system, the energy equation (46) must be added.

5. Modelling the gas neighbourhood of the particles

The goal of this section is to determine the values of mass fractions $Y^s_{CO_2}$, $Y^s_{O_2}$, $Y^s_{H_2O}$ and heat flux q''_p, at the surface of the particle, by modelling the gas environment outside the particle.

As the characteristic response time, $a^2/\mathcal{D}$, of the gas phase, at a distance r from the centre of the particle of the order of a, is short compared with the particle burning time, we are allowed to use the quasi-steady state approximation in the analysis of the gas phase response near the particle.

When analysing the gas neighbourhood of the particles, corresponding to $r > a$, the model described in the previous section remains valid with the exception that v_g is now the true velocity of the gas phase and $\mathcal{D}_e$ must be replaced by the gas phase diffusion coefficient $\mathcal{D}$. Furthermore, in equations (36)–(42), terms w_4 and w_5 do not appear. Hence, the conservation equations for the gas phase, in the neighbourhood of each particle, take the form

$$\rho_g v_g r^2 = \dot{m}, \tag{97}$$

$$\mathcal{L}(Y_{O_2}) = -\frac{4}{7}w_6 - \frac{32\nu_1}{M_{vol}}w_7 - 8w_8, \tag{98}$$

$$\mathcal{L}(Y_{CO_2}) = \frac{11}{7}w_6 + \frac{44\nu_2}{M_{vol}}w_7, \tag{99}$$

$$\mathcal{L}(Y_{H_2O}) = \frac{18\nu_3}{M_{vol}}w_7 + 9w_8, \tag{100}$$

$$\mathcal{L}(Y_{SO_2}) = \frac{64\nu_4}{M_{vol}} w_7, \tag{101}$$

$$\mathcal{L}(Y_{CO}) = -w_6, \tag{102}$$

$$\mathcal{L}(Y_V) = -w_7, \tag{103}$$

$$\mathcal{L}(Y_{H_2}) = -w_8, \tag{104}$$

$$\mathcal{L}(h_T) = q_6 w_6 + q_7 w_7 + q_8 w_8, \tag{105}$$

where $\mathcal{L}$ is defined as in (43), with $\mathcal{D}_e$ replaced by $\mathcal{D}$. These equations differ from the mean equations (8)–(16) for the gas phase environment in the elimination of the unsteady terms, the radiation term and the homogenized sources representing the effect of the particles.

Again, when solving the system of equations (98)–(105) in the limit of infinite Damköhler numbers for the gas phase reactions 6, 7 and 8, it is convenient to introduce the Schvab–Zeldovich combinations defined by equations (20)–(24), but now without the superscript g, so that the system of equations (98)–(105) will be replaced by

$$\mathcal{L}(\beta_i) = 0, \quad i = 1, \ldots, 4 \quad \text{and} \quad \mathcal{L}(H) = 0 \tag{106}$$

together with the Burke–Schumann equilibrium conditions

$$Y_{O_2} = 0, \quad \text{where } \beta_1 < 0 \tag{107}$$

and

$$Y_{CO} = Y_V = Y_{H_2} = 0, \quad \text{where } \beta_1 > 0. \tag{108}$$

In order to calculate Y_V, Y_{CO} and Y_{H_2} in the region $\beta_1 < 0$, we must solve, for example,

$$\mathcal{L}(Y_V) = 0 \quad \text{and} \quad \mathcal{L}(Y_{H_2}) = 0 \tag{109}$$

with conditions $Y_V = Y_{H_2} = 0$ where $\beta_1 = 0$.

The boundary conditions for this quasi-steady system of equations must first show that, at $r/a \to \infty$, the values of Y_α and h_T correspond to those of the ambient gas at the position occupied by the particle, namely

$$h_T = h_T^g \quad \text{and} \quad Y_\alpha = Y_\alpha^g, \quad \text{for } \alpha = O_2, CO_2, H_2O, SO_2, CO, V, H_2. \tag{110}$$

Notice that, even if we are interested in the steady operation of the furnace, these boundary conditions change with time because the particle is moving in the furnace. Actually, the values of Y_α^g and h_T^g are given by the gas flow model considered in Section 3, in terms of the position of the particle, as a function of time.

Moreover, at the particle surface, $r = a$, the mass fractions and temperature must be continuous as well as the mass fluxes due to convection and diffusion of each of the species. Global energy conservation at the interface requires the heat reaching the particle surface by conduction and radiation from the gas phase to enter the particle by heat conduction.

The solution of this system of equations is given below for three possible cases: in the first case there is no oxygen in the vicinity of the particle, i.e., the particle is in the domain Ω_F. In the other two cases, the particle lies in the domain Ω_O so that there is oxygen in its environment; then the volatiles, CO and H_2 generated within the particle are consumed in a flame sheet which lies outside the particle if $\beta_1^s < 0$, and inside the particle if $\beta_1^s > 0$.

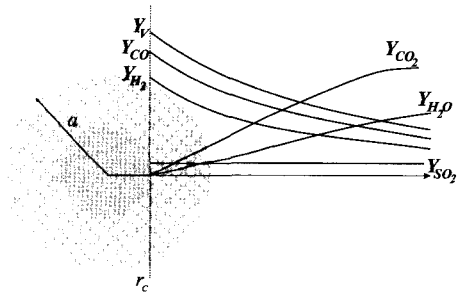

Figure 3. Coal particle in the domain Ω_F ($Y^g_{O_2} = 0$).

5.1 *First case: $Y^g_{O_2} = 0$, corresponding to the domain Ω_F, where $\beta^g_l < 0$*

In this case $Y_{O_2} = 0$ everywhere (see figure 3). Moreover the right-hand sides of the gas phase equations (99)–(105) vanish, because $w_6 = w_7 = w_8 = 0$. In particular we need to solve

$$\mathcal{L}(Y_{CO_2}) = \mathcal{L}(Y_{H_2O}) = \mathcal{L}(h_T) = 0 \tag{111}$$

with the boundary conditions given in (110), and

$$\begin{aligned} \dot{m}Y_{CO_2} - r^2\rho_g\mathcal{D}\frac{dY_{CO_2}}{dr}_{|r=a^+} &= -\frac{11}{3}\dot{m}_1, \\ \dot{m}Y_{H_2O} - r^2\rho_g\mathcal{D}\frac{dY_{H_2O}}{dr}_{|r=a^+} &= \dot{m}_5 - \frac{3}{2}\dot{m}_3, \\ \dot{m}h_T - r^2\rho_g\mathcal{D}\frac{dh_T}{dr}_{|r=a^+} &= \dot{m}h^s_T - a^2q''_g \end{aligned} \tag{112}$$

at the surface of the particle. Assuming $\rho_g\mathcal{D}$ is constant, the solution leads to the following values

$$Y^s_{CO_2} = Y_{CO_2}(a) = Y^g_{CO_2}e^{-\lambda} - \frac{11}{3}\frac{\lambda_1}{\lambda}(1 - e^{-\lambda}), \tag{113}$$

$$Y^s_{H_2O} = Y_{H_2O}(a) = Y^g_{H_2O}e^{-\lambda} + \left(\frac{\lambda_5}{\lambda} - \frac{3}{2}\frac{\lambda_3}{\lambda}\right)(1 - e^{-\lambda}), \tag{114}$$

$$q''_p = q''_g = \frac{k}{ac_p}(h^g_T - h^s_T)\frac{\lambda}{e^{\lambda} - 1}, \tag{115}$$

for the mass fractions of CO_2 and H_2O at the surface of the particle, and q''_g, the heat reaching the gas phase from the particle by conduction.

These relations are to be added to system (86)–(87), (81), (90)–(91), (95)–(96) and

$$\frac{4}{3}\pi a^3\rho_p c_s\frac{dT_p}{dt} = 4\pi a^2(q''_p + q''_r) + 4\pi\rho_g a\mathcal{D}(q_1\lambda_1 + q_3\lambda_3 + q_4\lambda_4 + q_5\lambda_5). \tag{116}$$

5.2 *Particle with a surrounding diffusion flame: $\beta^s_l < 0$ and $\beta^g_l > 0$*

Since $Y^g_{O_2} \neq 0$, then $Y^g_V = Y^g_{CO} = Y^g_{H_2} = 0$, because the gas phase reactions, being infinitely fast, do not allow the coexistence of oxygen with volatiles, H_2 and CO. The flame sheet lies where $\beta_1 = 0$ at $r = r_f > a$, and then $Y^s_{O_2} = 0$ (see figure 4).

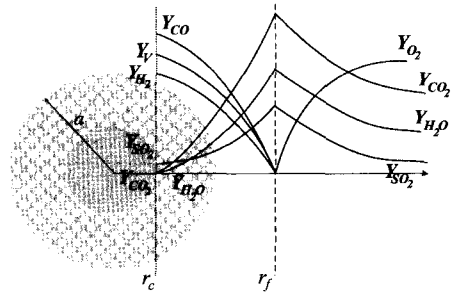

Figure 4. There is a separated flame in the vicinity of the particle.

In this case, the boundary conditions at the surface of the particle, $r = a$, are

$$\begin{aligned} \dot{m}Y_{CO_2} - r^2\rho_g\mathcal{D}\frac{dY_{CO_2}}{dr}_{|r=a^+} &= -\frac{11}{3}\dot{m}_1, \\ \dot{m}Y_{H_2O} - r^2\rho_g\mathcal{D}\frac{dY_{H_2O}}{dr}_{|r=a^+} &= \dot{m}_5 - \frac{3}{2}\dot{m}_3, \\ \dot{m}h_T - r^2\rho_g\mathcal{D}\frac{dh_T}{dr}_{|r=a^+} &= \dot{m}h_T^s - a^2q_g''. \end{aligned} \tag{117}$$

Assuming $\rho_g\mathcal{D}$ is constant, we can integrate (106) using the boundary conditions (117) at $r = a$ and (110) at $r \to \infty$. Then we obtain $Y_{O_2}(r)$, $Y_{CO_2}(r)$ and $Y_{H_2O}(r)$ in terms of $Y_{CO}(r)$, $Y_{H_2}(r)$ and $Y_V(r)$. We also need to calculate Y_V, Y_{H_2} and Y_{CO} in (a, r_f), by solving two of the conservation equations for Y_V, Y_{H_2} or Y_{CO} in the domain $a < r < r_f$, where w_6, w_7 and w_8 do not appear, and then using (50).

We thus obtain the following values of the mass fractions of O_2, CO_2 and H_2O, and the heat flux q_g'', at the surface of the particle:

$$Y_{O_2}^s = 0, \tag{118}$$

$$Y_{CO_2}^s = Y_{CO_2}^g e^{-\lambda} + \left(-\frac{11}{3} + \frac{11}{3}e^{-\lambda} + \frac{22}{3}e^{-\lambda}\varphi\right)\frac{\lambda_1}{\lambda} + \frac{11}{3}\frac{\lambda_3}{\lambda}e^{-\lambda}\varphi + \frac{44\nu_2}{M_{vol}}\frac{\lambda_4}{\lambda}e^{-\lambda}\varphi, \tag{119}$$

$$Y_{H_2O}^s = Y_{H_2O}^g e^{-\lambda} + \left(\frac{\lambda_5}{\lambda} - \frac{3}{2}\frac{\lambda_3}{\lambda}\right)(1 - e^{-\lambda}) + \left(\frac{3}{2}\frac{\lambda_3}{\lambda} + \frac{18\nu_3}{M_{vol}}\frac{\lambda_4}{\lambda}\right)e^{-\lambda}\varphi, \tag{120}$$

$$q_p'' = q_g'' = \frac{k}{ac_p}\frac{\lambda}{e^{\lambda} - 1}\left\{h_T^g - h_T^s + \left[q_6\left(\frac{14}{3}\frac{\lambda_1}{\lambda} + \frac{7}{3}\frac{\lambda_3}{\lambda}\right) + q_7\frac{\lambda_4}{\lambda} + q_8\frac{1}{6}\frac{\lambda_3}{\lambda}\right]\varphi\right\}, \tag{121}$$

and the position, r_f, of the diffusion flame is given by

$$r_f = \frac{\lambda a}{\ln(\varphi + 1)} \tag{122}$$

with

$$\varphi = \frac{Y_{O_2}^g}{\frac{8}{3}\left(\frac{\lambda_1}{\lambda} + \frac{\lambda_3}{\lambda}\right) + \frac{32\nu_1}{M_{vol}}\frac{\lambda_4}{\lambda}}. \tag{123}$$

These relations are to be added to system (86)–(87), (81), (90)–(91), (95)–(96) and

$$\frac{4}{3}\pi a^3\rho_p c_s\frac{dT_p}{dt} = 4\pi a^2(q_p'' + q_r'') + 4\pi\rho_g a\mathcal{D}\left(q_1\lambda_1 + q_3\lambda_3 + q_4\lambda_4 + q_5\lambda_5 + \frac{14}{3}q_6\lambda_1 + \frac{7}{3}q_6\lambda_3 + q_7\lambda_4 + \frac{1}{6}q_8\lambda_3\right). \tag{124}$$

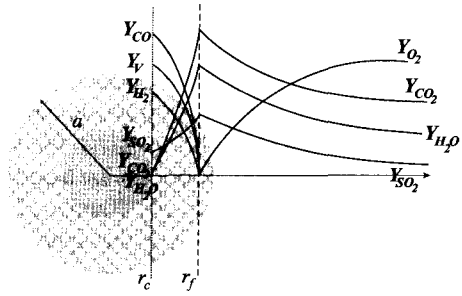

Figure 5. There is a flame inside the particle

5.3 *Flame sheet inside the particle: $\beta_i^s > 0$ when $r_c < r_f \leq a$*

In this section we consider the case where the infinitely fast reactions 6, 7 and 8 take place inside the particle, i.e. $r_c < r_f \leq a$ (see figure 5). In this case $Y_V = Y_{CO} = Y_{H_2} = 0$, for $r \geq a$, and the gas phase equations for O_2, CO_2, H_2O and the thermal enthalpy become

$$\mathcal{L}(Y_{O_2}) = \mathcal{L}(Y_{CO_2}) = \mathcal{L}(Y_{H_2O}) = \mathcal{L}(h_T) = 0 \tag{125}$$

because no reactions take place in the gas. Moreover, the boundary conditions at the surface of the particle are (110) and

$$\begin{aligned}
\dot{m}Y_{O_2} - r^2\rho_g\mathcal{D}\frac{dY_{O_2}}{dr}_{|r=a^+} &= -\frac{8}{3}(\dot{m}_1 + \dot{m}_3) - \frac{32\nu_1}{M_{vol}}\dot{m}_4,\\
\dot{m}Y_{CO_2} - r^2\rho_g\mathcal{D}\frac{dY_{CO_2}}{dr}_{|r=a^+} &= \frac{11}{3}(\dot{m}_1 + \dot{m}_3) + \frac{44\nu_2}{M_{vol}}\dot{m}_4,\\
\dot{m}Y_{H_2O} - r^2\rho_g\mathcal{D}\frac{dY_{H_2O}}{dr}_{|r=a^+} &= \dot{m}_5 + \frac{18\nu_3}{M_{vol}}\dot{m}_4,\\
\dot{m}h_T - r^2\rho_g\mathcal{D}\frac{dh_T}{dr}_{|r=a^+} &= \dot{m}h_T^s - a^2q_g''.
\end{aligned} \tag{126}$$

Now equations (125) can be integrated, using (126) and the boundary conditions at infinity obtaining

$$Y_{O_2}^s = Y_{O_2}^g e^{-\lambda} - \left[\frac{8}{3}\left(\frac{\lambda_1}{\lambda} + \frac{\lambda_3}{\lambda}\right) + \frac{32\nu_1}{M_{vol}}\frac{\lambda_4}{\lambda}\right](1 - e^{-\lambda}), \tag{127}$$

$$Y_{CO_2}^s = Y_{CO_2}^g e^{-\lambda} + \left[\frac{11}{3}\left(\frac{\lambda_1}{\lambda} + \frac{\lambda_3}{\lambda}\right) + \frac{44\nu_2}{M_{vol}}\frac{\lambda_4}{\lambda}\right](1 - e^{-\lambda}), \tag{128}$$

$$Y_{H_2O}^s = Y_{H_2O}^g e^{-\lambda} + \left(\frac{\lambda_5}{\lambda} + \frac{18\nu_3}{M_{vol}}\frac{\lambda_4}{\lambda}\right)(1 - e^{-\lambda}), \tag{129}$$

$$q_p'' = q_g'' = \frac{k}{ac_p}(h_T^g - h_T^s)\frac{\lambda}{e^{\lambda} - 1}. \tag{130}$$

These relations are to be added to system (75)–(80), with $\lambda_2 = 0$, (81), (90)–(91), (95)–(96) and

$$\begin{aligned}
\frac{4}{3}\pi a^3\rho_p c_s\frac{dT_p}{dt} &= 4\pi a^2(q_p'' + q_r'') + 4\pi\rho_g a\mathcal{D}(q_1\lambda_1 + q_3\lambda_3 + q_4\lambda_4 + q_5\lambda_5\\
&\quad + \frac{14}{3}q_6\lambda_1 + \frac{7}{3}q_6\lambda_3 + q_7\lambda_4 + \frac{1}{6}q_8\lambda_3).
\end{aligned} \tag{131}$$

Notice that, when $Y^g_{O_2} \to 0$, the parameter φ defined in (123) also tends to zero, which implies that $r_f \to \infty$. Then CO, H_2 and the volatiles do not burn in the vicinity of the particle; they are consumed in the gaseous diffusion-controlled flames, Γ_F, bounding the region without oxygen (see Section 3). The particle response, when it lies in the region Ω_F where $Y^g_{O_2} = 0$, has been analysed in Section 5.1.

The analyses carried out in the two previous subsections are based on the assumption that the Damköhler numbers, or ratios of the diffusion times, $a^2/\mathcal{D}$ and $a^2/\mathcal{D}_e$, and the chemical times, are large compared with unity; notice that the diffusivity that appears here is often significantly larger than the diffusivity $\mathcal{D}_e$ inside the porous particle[1] (when dealing with volatiles, like CH_4, combustion requires a significant large amount of air to burn in a stoichiometric mixture, so the diffusion flame will lie at a distance r_f large compared with a, and then the appropriate diffusion time, $r_f^2/\mathcal{D}$, is much larger than $a^2/\mathcal{D}$, making it easier to satisfy the above Burke–Schumann assumption).

When the Damköhler numbers are large the reaction layers, where the reactants coexist, are thin compared with the particle radius, thus justifying the Burke–Schumann assumption. If the Damköhler numbers decrease to values of order unity (for example because of the decreasing values of the particle size) the reaction thickness, measured with the particle size, will grow. For smaller values of particle, the volatiles, CO and H_2 will eventually burn where the ambient gas temperature is large enough to ensure that the Damköhler number associated with the homogenized gas phase is large.

Thus, if we use the Burke–Schumann assumption in cases where the relevant Damköhler number for combustion near the particle is small, we simply over-predict the rate of gasification of the particle without changing otherwise the homogenized CO_2, H_2O and energy release.

Anyway, we shall give a more accurate description of the particle gasification rate, when the Damköhler number based on the size of the particle is small but the Damköhler number associated with the homogenized gas phase is large. Then, the gas phase oxidation reactions of the volatiles, CO and H_2 can be considered as frozen inside the particle or in its vicinity, and they will only take place in extended reaction zones, with small values of the mass fractions of the volatiles, CO and H_2 and also small changes of Y_{O_2} and $Y^g_{O_2}$. In this case, oxygen can reach the surface of the particle and contribute to the char gasification. A similar analysis to the one given previously in Section 5.1 leads to

$$\frac{11}{3}\frac{\lambda_1}{\lambda} = \left\{ Y^g_{CO_2} + \frac{11}{3}\frac{\lambda_1}{\lambda} \right\} e^{\lambda \frac{\mathcal{D}}{\mathcal{D}_e}(1-a/r_c)-\lambda}, \tag{132}$$

$$\frac{4}{3}\frac{\lambda_2}{\lambda} = \left\{ Y^g_{O_2} + \frac{4}{3}\frac{\lambda_2}{\lambda} \right\} e^{\lambda \frac{\mathcal{D}}{\mathcal{D}_e}(1-a/r_c)-\lambda}, \tag{133}$$

$$\frac{3}{2}\frac{\lambda_3}{\lambda} - \frac{\lambda_5}{\lambda} = \left\{ Y^g_{H_2O} + \frac{3}{2}\frac{\lambda_3}{\lambda} - \frac{\lambda_5}{\lambda} \right\} e^{\lambda \frac{\mathcal{D}}{\mathcal{D}_e}(1-a/r_c)-\lambda}, \tag{134}$$

$$\frac{\rho^0_C}{\rho_g a \mathcal{D}} r_c^2 \frac{dr_c}{dt} = -(\lambda_1 + \lambda_2 + \lambda_3). \tag{135}$$

In order to obtain a closed system, we must add equations (90)–(91), (95)–(96) and the energy equation

$$\frac{4}{3}\pi a^3 \rho_p c_s \frac{dT_p}{dt} = 4\pi a^2 (q''_p + q''_r) + 4\pi \rho_g a \mathcal{D}(q_1\lambda_1 + q_2\lambda_2 + q_3\lambda_3 + q_4\lambda_4 + q_5\lambda_5). \tag{136}$$

---

[1] For an estimate of the value of the reaction time outside the particle we can use the diffusion time, $\delta_L^2/\mathcal{D}$, across the flame thickness δ_L of the stoichiometric mixture of the reactant and oxidizer (where typically δ_L is of order of 50 μm).

Finally, it is obvious that the Burke–Schumann assumption prevents us from describing regions of low gas temperature near the injector, where the quenching of the diffusion flames surrounding the small particles would result in the coexistence in the homogenized gas phase of oxygen with volatiles, CO and H_2, with significant concentrations of these species if the mean gas phase Damköhler numbers are not large, which will finally burn with the oxygen in gas phase premixed flames.

6. Sources to the gas phase from one single particle

In this section we write the expressions of the sources of mass and energy to the gas phase from one single particle, in the three cases considered in Section 5. It must be taken into account that $\lambda_2 \neq 0$ only in the limit case when reactions 1, 2 and 3 are kinetically controlled or when oxygen reaches the particle core surface because of the small particle size based Damköhler numbers.

The sources of mass of each of the species due to one particle are:

1. In Ω_F ($\beta_1^g < 0$ or $Y_{O_2}^g = 0$):

$$F_{O_2}^m = F_{SO_2}^m = 0, \tag{137}$$

$$F_{CO_2}^m = \frac{4\pi ak}{c_p}\left(-\frac{11}{3}\lambda_1\right), \tag{138}$$

$$F_{H_2O}^m = \frac{4\pi ak}{c_p}\left(\lambda_5 - \frac{3}{2}\lambda_3\right), \tag{139}$$

$$F_{CO}^m = \frac{4\pi ak}{c_p}\left(\frac{14}{3}\lambda_1 + \frac{7}{3}\lambda_3\right), \tag{140}$$

$$F_V^m = \frac{4\pi ak}{c_p}\lambda_4, \tag{141}$$

$$F_{H_2}^m = \frac{4\pi ak}{c_p}\frac{1}{6}\lambda_3. \tag{142}$$

2. In Ω_O ($\beta_1^g > 0$ or $Y_{O_2}^g \neq 0$), when the Damköhler numbers based on the particle size are large:

$$F_{O_2}^m = \frac{4\pi ak}{c_p}\left(-\frac{8}{3}(\lambda_1 + \lambda_3) - \frac{32\nu_1}{M_{vol}}\lambda_4\right), \tag{143}$$

$$F_{CO_2}^m = \frac{4\pi ak}{c_p}\left(\frac{11}{3}(\lambda_1 + \lambda_3) + \frac{44\nu_2}{M_{vol}}\lambda_4\right), \tag{144}$$

$$F_{H_2O}^m = \frac{4\pi ak}{c_p}\left(\lambda_5 + \frac{18\nu_3}{M_{vol}}\lambda_4\right), \tag{145}$$

$$F_{SO_2}^m = \frac{4\pi ak}{c_p}\frac{64\nu_4}{M_{vol}}\lambda_4, \tag{146}$$

$$F_{CO}^m = F_V^m = F_{H_2}^m = 0, \tag{147}$$

whereas, when these Damköhler numbers are small:

$$F^{\mathrm{m}}_{\mathrm{O}_2} = \frac{4\pi ak}{c_p}\left(-\frac{4}{3}\lambda_2\right), \tag{148}$$

$$F^{\mathrm{m}}_{\mathrm{CO}_2} = \frac{4\pi ak}{c_p}\left(-\frac{11}{3}\lambda_1\right), \tag{149}$$

$$F^{\mathrm{m}}_{\mathrm{H_2O}} = \frac{4\pi ak}{c_p}\left(\lambda_5 - \frac{3}{2}\lambda_3\right), \tag{150}$$

$$F^{\mathrm{m}}_{\mathrm{SO}_2} = 0, \tag{151}$$

$$F^{\mathrm{m}}_{\mathrm{CO}} = \frac{4\pi ak}{c_p}\left(\frac{14}{3}\lambda_1 + \frac{7}{3}\lambda_2 + \frac{7}{3}\lambda_3\right), \tag{152}$$

$$F^{\mathrm{m}}_{\mathrm{V}} = \frac{4\pi ak}{c_p}\lambda_4, \tag{153}$$

$$F^{\mathrm{m}}_{\mathrm{H}_2} = \frac{4\pi ak}{c_p}\left(\frac{1}{6}\lambda_3\right). \tag{154}$$

In all of the cases, the total source of mass from the particle to the gas is given by

$$F^{\mathrm{m}} = \frac{4\pi ak}{c_p}\lambda \tag{155}$$

and the source of energy is

$$F^{\mathrm{e}} = 4\pi ak\left\{\left(\frac{c_s}{c_p}T_p - T_g\right)\frac{\lambda}{e^{\lambda}-1} + (1-\vartheta)\left[\frac{q_6}{c_p}\left(\frac{14}{3}\lambda_1 + \frac{7}{3}\lambda_3\right) + \frac{q_7}{c_p}\lambda_4 + \frac{q_8}{c_p}\frac{1}{6}\lambda_3\right]\right\} - c_s T_p\frac{dm_p}{dt}, \tag{156}$$

where $m_p = \frac{4}{3}\pi a^3\rho_p$ and

$$\vartheta = \begin{cases} 1 & \text{when } \beta_1^s > 0 \text{ (flame sheet inside the particle), } \beta_1^g < 0 \text{ (no oxygen in the vicinity) or when } \beta_1^g > 0 \text{ but, oxygen reaches the particle core surface because of the small particle size based Damköhler numbers,} \\ \dfrac{\varphi}{e^{\lambda}-1} & \text{when } \beta_1^g > 0 \text{ and } \beta_1^s < 0 \text{ (flame sheet outside the particle).} \end{cases}$$

Finally, the homogenized sources in the gas phase per unit volume and time, at point x of the boiler, are obtained from the individual sources of one particle by

$$f^{\alpha}(x) = \sum_{j=1}^{N_e}\sum_{i=1}^{N_p}\tilde{q}_j\frac{p_{ij}}{100}\int_0^{t_f^{ij}} F_{ij}^{\alpha}(t)\delta(x - x_s^{ij}(t))dt \tag{157}$$

where $F_{ij}^{\alpha}(t)$ denotes the contribution of one individual particle of type i introduced through inlet j, at instant t (given by expressions (137)–(156)), $x_s^{ij}(t)$ is the position occupied by this particle at instant t, $\delta(x)$ is the Dirac measure at point 0, t_f^{ij} is the time needed for the particle to be completely burned or to leave the furnace, $\tilde{q}_j$ is the mass flow of coal through inlet j, p_{ij} is the percentage of particles of type i through inlet j, and N_e and N_p are the number of inlets and types of particles, respectively.

7. Summary of the relations given the non-dimensional gasification rates

In this section we summarize the relations determining the non-dimensional gasification rates λ_i and, thereby, the sources F^m given by equations (137)–(156). They characterize the particle response obtained in the Sections 4 and 5, when considering the case of large Damköhler numbers ($Da_i \gg 1, i = 1, 2, 3$).

When the particle lies in Ω_F, we have obtained

$$\begin{aligned}
\frac{11}{3}\frac{\lambda_1}{\lambda} &= \left\{Y^g_{CO_2} + \frac{11}{3}\frac{\lambda_1}{\lambda}\right\} e^{\lambda \frac{\mathcal{D}}{\mathcal{D}_e}(1-a/r_c)-\lambda}, \\
\frac{3}{2}\frac{\lambda_3}{\lambda} - \frac{\lambda_5}{\lambda} &= \left\{Y^g_{H_2O} + \frac{3}{2}\frac{\lambda_3}{\lambda} - \frac{\lambda_5}{\lambda}\right\} e^{\lambda \frac{\mathcal{D}}{\mathcal{D}_e}(1-a/r_c)-\lambda}, \\
\frac{\rho^0_C}{\rho_g a \mathcal{D}} r_c^2 \frac{dr_c}{dt} &= -(\lambda_1 + \lambda_3).
\end{aligned} \tag{158}$$

The relations determining the gasification rates are similar when the particles lies in the region Ω_O, if the Damköhler numbers for the gas phase oxidation reactions based on the particle size are small compared to unity, because then these reactions will only take place far from the particle in the homogenized gas phase with small values of the concentrations of the volatiles, H_2 and CO. In that case we have obtained

$$\begin{aligned}
\frac{11}{3}\frac{\lambda_1}{\lambda} &= \left\{Y^g_{CO_2} + \frac{11}{3}\frac{\lambda_1}{\lambda}\right\} e^{\lambda \frac{\mathcal{D}}{\mathcal{D}_e}(1-a/r_c)-\lambda}, \\
\frac{4}{3}\frac{\lambda_2}{\lambda} &= \left\{Y^g_{O_2} + \frac{4}{3}\frac{\lambda_2}{\lambda}\right\} e^{\lambda \frac{\mathcal{D}}{\mathcal{D}_e}(1-a/r_c)-\lambda}, \\
\frac{3}{2}\frac{\lambda_3}{\lambda} - \frac{\lambda_5}{\lambda} &= \left\{Y^g_{H_2O} + \frac{3}{2}\frac{\lambda_3}{\lambda} - \frac{\lambda_5}{\lambda}\right\} e^{\lambda \frac{\mathcal{D}}{\mathcal{D}_e}(1-a/r_c)-\lambda}, \\
\frac{\rho^0_C}{\rho_g a \mathcal{D}} r_c^2 \frac{dr_c}{dt} &= -(\lambda_1 + \lambda_2 + \lambda_3).
\end{aligned} \tag{159}$$

The analysis of the situations when particle lies in region Ω_O and the Damköhler numbers for the gas phase oxidation reactions based on the particle size are large is more complicated. Thus, when the particle lies in Ω_O and as long as $Y^s_{O_2}$ given by (127) is larger than zero, so that $r_c < r_f \leq a$, we have obtained

$$\begin{aligned}
& e^{\lambda \frac{\mathcal{D}}{\mathcal{D}_e}(a/r_f - 1)+\lambda} = \varphi + 1, \\
& \frac{11}{3}\frac{\lambda_1}{\lambda} - \left[\frac{22}{3}\frac{\lambda_1}{\lambda} + \frac{11}{3}\frac{\lambda_3}{\lambda} + \frac{44\nu_2}{M_{vol}}\frac{\lambda_4}{\lambda}\right] e^{\lambda \frac{\mathcal{D}}{\mathcal{D}_e}(a/r_f - a/r_c)} \\
& \quad = \left\{Y^g_{CO_2} - \frac{11}{3}\left(\frac{\lambda_1}{\lambda} + \frac{\lambda_3}{\lambda}\right) - \frac{44\nu_2}{M_{vol}}\frac{\lambda_4}{\lambda}\right\} e^{\lambda \frac{\mathcal{D}}{\mathcal{D}_e}(1-a/r_c)-\lambda}, \\
& \frac{3}{2}\frac{\lambda_3}{\lambda} - \frac{\lambda_5}{\lambda} - \left(\frac{3}{2}\frac{\lambda_3}{\lambda} + \frac{18\nu_3}{M_{vol}}\frac{\lambda_4}{\lambda}\right) e^{\lambda \frac{\mathcal{D}}{\mathcal{D}_e}(a/r_f - a/r_c)} = \left\{Y^g_{H_2O} - \frac{\lambda_5}{\lambda} - \frac{18\nu_3}{M_{vol}}\frac{\lambda_4}{\lambda}\right\} e^{\lambda \frac{\mathcal{D}}{\mathcal{D}_e}(1-a/r_c)-\lambda}, \\
& \frac{\rho^0_C}{\rho_g a \mathcal{D}} r_c^2 \frac{dr_c}{dt} = -(\lambda_1 + \lambda_3),
\end{aligned} \tag{160}$$

with φ given by (123).

When the particle lies in Ω_O and $r_f > a$, we have obtained

$$\frac{11}{3}\frac{\lambda_1}{\lambda} = \left\{Y^g_{CO_2} + \frac{11}{3}\frac{\lambda_1}{\lambda} + \left(\frac{22}{3}\frac{\lambda_1}{\lambda} + \frac{11}{3}\frac{\lambda_3}{\lambda} + \frac{44\nu_2}{M_{vol}}\frac{\lambda_4}{\lambda}\right)\varphi\right\} e^{\lambda\frac{D}{D_c}(1-a/r_c)-\lambda},$$

$$\frac{3}{2}\frac{\lambda_3}{\lambda} - \frac{\lambda_5}{\lambda} = \left\{Y^g_{H_2O} + \frac{3}{2}\frac{\lambda_3}{\lambda} - \frac{\lambda_5}{\lambda} + \left(\frac{3}{2}\frac{\lambda_3}{\lambda} + \frac{18\nu_3}{M_{vol}}\frac{\lambda_4}{\lambda}\right)\varphi\right\} e^{\lambda\frac{D}{D_c}(1-a/r_c)-\lambda}, \tag{161}$$

$$\frac{\rho^0_C}{\rho_g a\mathcal{D}} r_c^2 \frac{dr_c}{dt} = -(\lambda_1 + \lambda_3),$$

with φ given by (123) or, equivalently, $\varphi = e^{\lambda a/r_f} - 1$.

Moreover, one can prove that the resulting equations (160), corresponding to the flame sheet inside the particle ($r_f < a$), coincides with the equations (161), corresponding to the flame sheet outside the particle but in its neighbourhood ($r_f > a$), when $r_f = a$; thus ensuring the continuity of both systems. In the same way, in the limit $r_f \to \infty$, equations (161) tends to the equations (158), corresponding to the particle burning in the zone where is no oxygen, i.e. $\beta^g_1 < 0$. This also leads to the continuity of both systems.

8. Concluding remarks

In this paper we have introduced a mathematical model which can be used to simulate combustion in pulverized coal furnaces.

A homogenized model has been built for the gas phase with the effect of particles represented by volumetric sources of heat, mass and momentum. Analytical expressions of these sources have been obtained by analysing the Lagrangian response of a coal particle in the variable gas environment seen by the particle during its lifetime. For this purpose we have accounted for the overlapping of the evaporation and devolatilization reactions, producing water vapour and a generic reacting volatile, and the char gasification which generates CO and H_2, by the heterogeneous reactions of the carbon with O_2, CO_2 or H_2O.

We have also accounted for the gas phase oxidation of CO, H_2 and the volatiles, assuming these reactions with oxygen to be infinitely fast. This assumption allows us to describe the values of the gas phase temperature and concentrations in terms of Schvab–Zeldovich linear combinations of these variables, conserved by the gas phase reactions. With this assumption the mean gas phase value of one of these coupling functions determines the region, or regions, Ω_F of the flow field where there is no oxygen, and its boundary Γ_F which is the flame sheet where the reactants generated by the gasification of particles lying in Ω_F react with oxygen in the form of group combustion.

In the rest, Ω_O, of the flow field there is oxygen so that, if the characteristic Damköhler number based on the scales of the homogenized gas flow is large, then the reactants generated by the gasification of the particles lying in Ω_O must be consumed in the neighbourhood of the particles or in their near-wakes.

When we consider in this paper the particle size based Damköhler numbers of the gas phase reactions to be large, these reactions must occur in thin flame sheets inside the particles or outside, surrounding them. However for small particle size based Damköhler numbers, the above flame sheet model would overpredict the particle gasification rates. Thus, for a more accurate prediction of the particle gasification rate, the gas phase reactions have been considered as frozen when describing the gas properties inside and near the particles. In this case we must account for the effect of the reaction of the char with the oxygen that is now allowed to reach the particle.

In our analysis we have considered that the spatial variations of temperature are small within the particle and, when describing the evaporation and devolatilization reactions, and the oxidation of the char by CO_2, H_2O and O_2, we have used distributed reaction models. We have considered that the char gasification reactions have large activation energies, defining three Damköhler numbers, which are small compared with unity for values of the particle temperature T_p below a critical value, so that the char gasification can be neglected. For larger values of T_p the char gasification reactions occur in a diffusion controlled way, in a thin layer separating a shrinking core from a surrounding external ash layer. This introduces diffusion limitations to the supply of oxygen to the layer, which are accounted for in our analysis. In coals with low ash content the ash layer is not structurally stable, and the models where the char gasification occurs at the particle surface include a radius that decreases with time. The analysis of this case is simpler, and it can be carried out with the procedure used in this paper.

The description of the particle gasification requires the determination of the evolution of the temperature within the particle and the densities of the condensed volatiles, water vapour and char needs of the analysis of the gaseous neighbourhood of the particle. This analysis includes not only the heat reaching the particle by conduction from the gas phase and the mass fractions of CO_2 and O_2 at the particle surface, but also the sources from the particles affecting the gas phase temperature and concentrations. When during the particle response a shrinking core is encountered we must also determine the time evolution of its radius.